The Electric Field Response of the Van Veen Loop

James McLean[1], Koji Takizawa, Masataka Midori, Hiroshi Kurihara, and Robert Sutton

TDK Corp.
Tokyo, Japan and Cedar Park, Texas, USA
[1]jmclean@tdkrf.com

Abstract—**The Van Veen Loop, Large Loop Antenna (LLA), or Loop Antenna System (LAS), provides rapid determination of the net magnetic dipole moment of compact devices, especially in the frequency range of 9 kHz to 30 MHz, with minimal post processing of measured data. The symmetric shielded loop structure inherently rejects electric field excitation to a large extent if the action of the current transformer is ideal. Here we consider the electric-field or common-mode response of an LLA with an imperfect current transformer. The impetus for this work is the application of the LLA to the characterization of Inductive Power Transfer (IPT) systems. It has been shown that such IPT systems exhibit, in addition to an intense magnetic dipole moment, an intense electric dipole moment. This is due primarily to the turn-to-turn voltage drop in inductive couplers.**

I. Introduction

The Van Veen loop, Large Loop Antenna (LLA), or Loop Antenna System (LAS), provides an accurate assessment of the net vector dipole moment of a compact source of magnetic field interference [1]–[8]. The system consists of three orthogonal shielded loops each with two symmetrically-located feeds. These symmetrically-located feeds improve the rejection of electric field allowing accurate measurement of three orthogonal vector components of magnetic dipole moment, even in the presence of intense electric field. It is, however, not only the shielded structure but also the current sensing transformer that ultimately provides electric field rejection as will be clarified here.

II. 3-Port Model for Current Transformer

In refs. [1]–[8], the current transformer is treated as an ideal current transformer modeled by a transimpedance, the ratio of output voltage to input current and an insertion impedance, and the effective impedance inserted into the LLA. The non-ideal current transformer necessarily requires a more complex representation. We note that the current transformer specified in ref. [4] is fully enclosed by a shield with three coaxial ports each having a coaxial connecter. Thus, it is not only sound to consider the transformer as a 3-port network, it is also possible to measure the 3-port network parameters using a conventional network analyzer. The analytical 3-port model for the current transformer is useful for understanding the asymmetry introduced by the inter-winding capacitance. Referring to Fig. 1, in the absence of inter-winding capacitance and turn-to-turn capacitance, the 3-port admittance matrix of

the current transformer is:

$$[Y_T] = \left(j\omega L_1 + \frac{\omega^2 M^2}{j\omega L_2}\right)^{-1} \begin{bmatrix} 1 & -1 & -\frac{M}{L_2} \\ -1 & 1 & \frac{M}{L_2} \\ -\frac{M}{L_2} & \frac{M}{L_2} & \frac{L_2}{L_1} \end{bmatrix} \quad (1)$$

where L_1 is the self inductance of the primary, L_2 is the self inductance of the secondary, and M is the mutual inductance. Note that $Y_{31} = -Y_{32}$. This provides current balun behavior in the current transformer [9]; that is, since $Y_{11} = Y_{22}$, if the transformer is driven from port 3, $I_2 = -I_1$. In current sensing operation, the output is proportional to $I_1 - I_2$. Thus, the transformer does not respond at all to common-mode excitation. When inter-winding capacitance is present,
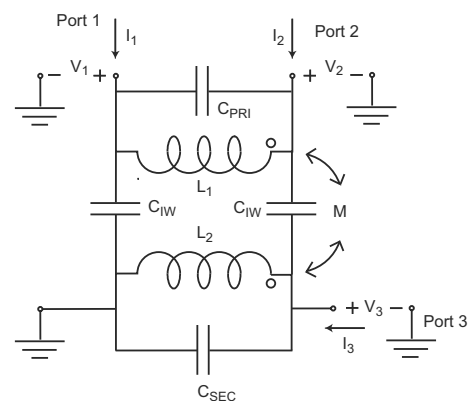

Fig. 1. Detailed circuit model for current transformer including inter-winding capacitance and turn-to-turn capacitance. The inter-winding capacitance destroys the symmetry of the admittance matrix and introduces common-mode response.

it is straightforward to derive the admittance matrix using the indefinite admittance matrix approach. The unique entries of

the admittance matrix are:

$$Y_{T11} = \left[Z_{pri} + \frac{\omega^2 M^2}{Z_{sec}} \right]^{-1} + j\omega C_{IW}, \qquad (2)$$

$$Y_{T22} = Y_{11}, \qquad (3)$$

$$Y_{T33} = \left[Z_{sec} + \frac{\omega^2 M^2}{Z_{pri}} \right]^{-1} + j\omega C_{IW}, \qquad (4)$$

$$Y_{T21} = -\left[Z_{pri} + \frac{\omega^2 M^2}{Z_{sec}} \right]^{-1}, \qquad (5)$$

$$Y_{T31} = \left(\frac{j\omega M}{Z_{sec}} \right) \left[Z_{pri} + \frac{\omega^2 M^2}{Z_{sec}} \right]^{-1}, \text{ and} \qquad (6)$$

$$Y_{T32} = -\left(\frac{j\omega M}{Z_{sec}} \right) \left[Z_{pri} + \frac{\omega^2 M^2}{Z_{sec}} \right]^{-1} - j\omega C_{IW}, (7)$$

where $Z_{pri} = j\omega L_1 || \frac{1}{j\omega C_{PRI}}$, $Z_{sec} = j\omega L_2 || \frac{1}{j\omega C_{SEC}}$. As shown in Fig. 1, C_{SEC} approximately represents the turn-to-turn distributed capacitance of the 25-turn secondary, which can be significant at the upper end of the 9 kHz to 30 MHz frequency range. On the other hand, the primary has a single turn consisting of the center conductor of the coaxial line and the transformer housing or shield. Thus, the parallel capacitance is typically not significant in this frequency range. Since the transformer is reciprocal, the admittance matrix is symmetric about its principal diagonal. As can be seen by comparing Eqn. 1 to Eqn. 2-7, the inter-winding capacitance causes: $Y_{31} \neq -Y_{32}$. Additionally, the inter-winding capacitance affects the matrix elements on the principal diagonal, the self admittances. This modifies the overall frequency response, including to some extent the differential or current mode response. We can experimentally determine C_{IW} as:

$$-(Y_{31} + Y_{32}) = j\omega C_{IW}. \qquad (8)$$

Finally, we note that the inter-winding capacitance is related to the number of turns in the secondary; that is, it increases as the number of turns in the secondary is increased. However, the low-frequency limit of operation, the effective turns ratio, and the insertion impedance are set by the requirements in ref. [4], namely a transimpedance of 1 Ω and an operating frequency range of 9 kHz to 30 MHz. For this reason it is not possible to simply employ a small number of turns in the secondary to minimize parasitic behavior.

III. 3-Port Model for the LLA and Folded Dipole

A 3-port electromagnetic model for the combination of folded dipole and large loop was computed in ref. [8] using the Numerical Electromagnetics Code. Here we use exactly the same model, including the same orientation of the loop and the height of the loop above the ground plane. Thus, the results here can be compared directly to those in ref. [8]. The left and right ports of the loop are designated ports 1 and 2 respectively, while the port of the folded dipole is designated as port 3. The transfer admittances, Y_{31} and Y_{32} as computed from the NEC model in ref. [8], are shown in Fig. 2. As can be seen, $Y_{31} = -Y_{32}$ at low frequencies, but differ significantly near 30 MHz. This is due to the asymmetry

of the folded dipole feed. The asymmetry in the folded dipole feed is what is responsible for the excitation of electric dipole moment in the folded dipole structure. Despite the asymmetry
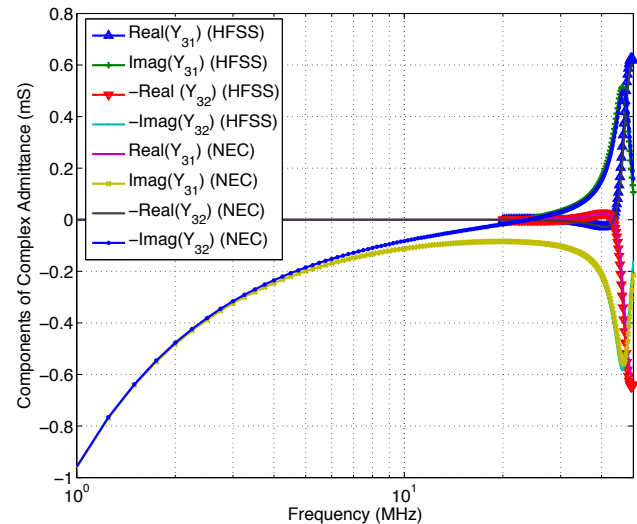

Fig. 2. Admittance parameters for folded-dipole, LLA combination as computed by NEC and the commercial finite element simulation HFSS. The arrangement is exactly the same as that used in ref. [8]. Note that the components $-Y_{32}$ are plotted to facilitate comparison. As can be seen the two different (MoM versus FEM) numerical simulations are in good agreement.

in the transfer admittances, the interior circuit of the LLA, if the LLA is symmetric, acts as a 1:1 current balun. The asymmetry in the transfer admittances cannot cause common-mode current to flow in the LLA if the current transformer acts as an ideal transformer. In ref. [8], the validation factor was computed by sampling the current at the midpoint of the lower half of the large loop. This is equivalent to having a perfect current transformer with a transimpedance of 1 Ω and negligible insertion impedance. Thus, despite the fact that the data in Fig. 2 is exactly the same data used in ref. [8], the results in ref. [8] do not reflect the common-mode or electric field response.

IV. Composite Admittance Matrix Representation

The interior structure of the LLA can be modeled systematically by building up a composite admittance matrix representation from the equivalent network in Fig. 3. In the analysis that follows, multi-port admittance parameters are defined with positive port current entering the terminal of the port with the positive voltage reference. The interior circuit can be modeled starting with the admittance matrix representation of a uniform transmission line:

$$[Y] = \begin{bmatrix} -jY_0 \cot\theta & jY_0 \csc\theta \\ jY_0 \csc\theta & -jY_0 \cot\theta \end{bmatrix}. \qquad (9)$$

Since the terminating resistors are situated across the left and right ports of the upper portion of the coaxial cable, the 2-port
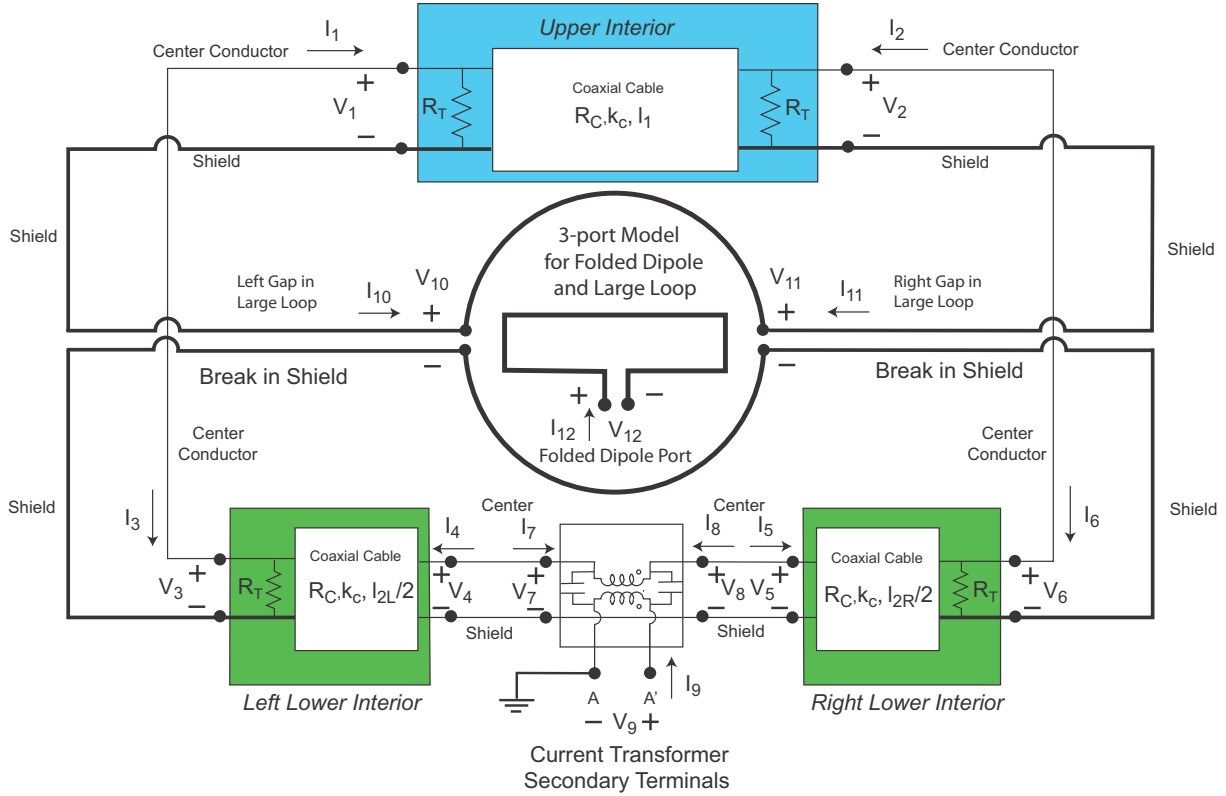
Fig. 3.   Generalized Equivalent Network for the Van Veen Antenna or Large Loop Antenna (LLA). The 3-port network parameters of the Van-Veen Loop exterior and DUT antenna (the folded dipole) can be computed using electromagnetic simulation. The 3-port transformer representation can be measured using a VNA since it has 3 coaxial ports. Note that Port 12 of the folded dipole implicitly contains a current balun representing the "infinite balun" structure by which the folded dipole is fed.

admittance matrix for the upper interior in Fig. 3 is:

$$
[Y_U] = \begin{bmatrix} G & 0 \\ 0 & 0 \end{bmatrix}
+ \begin{bmatrix} -jY_0\cot\theta_U & jY_0\csc\theta_U \\ jY_0\csc\theta_U & -jY_0\cot\theta_U \end{bmatrix}
+ \begin{bmatrix} 0 & 0 \\ 0 & G \end{bmatrix} \tag{10}
$$

where $\theta_U = l_1 k_C$, $Y_0 = \frac{1}{R_C}$, and $G = \frac{1}{R_T}$. Since a terminating resistor exists only across the left-hand port of the lower left portion of the coaxial cable, the 2-port admittance matrix for the lower left interior in Fig. 3 is:

$$
[Y_{LL}] = \begin{bmatrix} G & 0 \\ 0 & 0 \end{bmatrix}
+ \begin{bmatrix} -jY_0\cot\theta_{LL} & jY_0\csc\theta_{LL} \\ jY_0\csc\theta_{LL} & -jY_0\cot\theta_{LL} \end{bmatrix} \tag{11}
$$

where $\theta_{LL} = l_{2L} k_C$. Since a terminating resistor exists only across the right-hand port of the lower right portion of the coaxial cable, the 2-port admittance matrix for the lower right interior in Fig. 3 is:

$$
[Y_{LR}] = \begin{bmatrix} -jY_0\cot\theta_{LR} & jY_0\csc\theta_{LR} \\ jY_0\csc\theta_{LR} & -jY_0\cot\theta_{LR} \end{bmatrix}
+ \begin{bmatrix} 0 & 0 \\ 0 & G \end{bmatrix} \tag{12}
$$

where $\theta_{LR} = l_{2R} k_C$. The composite admittance matrix is thus:

$$
[Y] = \begin{bmatrix}
\underbrace{[Y_U]}_{2\times2} & [0] & [0] & [0] & [0] \\
[0] & \underbrace{[Y_{LL}]}_{2\times2} & [0] & [0] & [0] \\
[0] & [0] & \underbrace{[Y_{LR}]}_{2\times2} & [0] & [0] \\
[0] & [0] & [0] & \underbrace{[Y_T]}_{3\times3} & [0] \\
[0] & [0] & [0] & [0] & \underbrace{[Y_L]}_{3\times3}
\end{bmatrix} \tag{13}
$$

where Y_U is the 2-port admittance matrix representing the top portion of the coaxial line and terminating resistors, Y_{LL} is the 2-port admittance matrix representing the lower left portion of the coaxial line and terminating resistors, Y_{LR} is the 2-port admittance matrix representing the lower right portion of the coaxial line and terminating resistors, Y_T is the 3-port admittance matrix representing the current transformer in Eqns. 2-7, and Y_L is the 3-port admittance matrix representing the combination of the LLA and folded dipole as described in ref. [8]. At this point in the analysis, $I_1 \ldots I_{12}$ and $V_1 \ldots V_{12}$ are unknown. However, ports 4 and 7 are connected in parallel as are ports 8 and 5. Thus, $V_4 = V_7$, $V_5 = V_8$, $I_4 = -I_7$,

and $I_5 = -I_8$. The source in the CISPR 16-2-3 standard exhibits a 50 Ohm output impedance and the validation factor is defined as the ratio of loop current (assuming a perfect current transformer) to the source open circuit voltage, V_G. Therefore, we set $V_G = 1$ and thus: $V_{12} = 1 - R_G I_{12}$. Finally, a $R_L = 50 \ \Omega$ load is connected to port 9 and thus $V_9 = -R_L I_9$. Thus, a linear system can be set up and solved for V_9, the current transformer output.
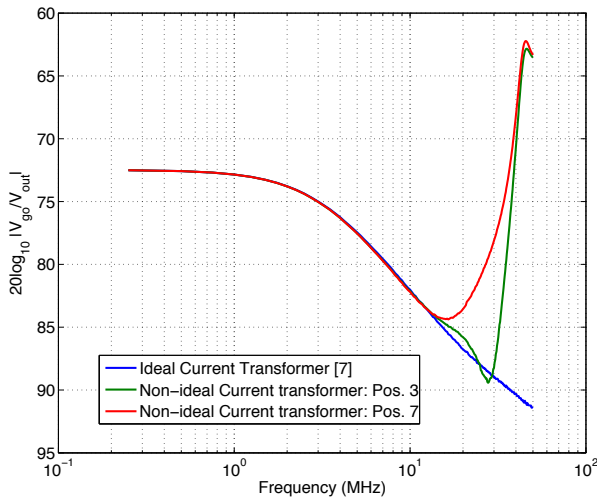
V. RESULTS FOR VALIDATION FACTOR

Fig. 4. Validation factor for 2 m diameter LLA as computed for an idealized LLA with an ideal current transformer (blue), and an idealized LLA and a non-ideal current transformer.
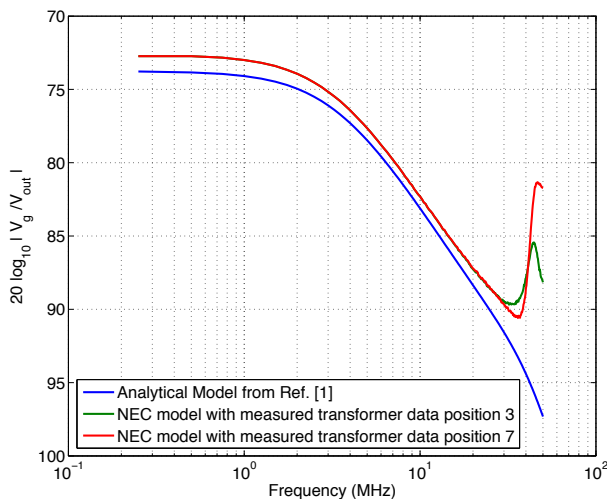

Fig. 5. Predicted value for $20 \log_{10} \left| \frac{V_{go}}{V_{out}} \right|$. The folded dipole and LLA combination was simulated by NEC. The arrangement is exactly the same as that used in ref. [8]. The data for the current transformer was measured.

Predictions of the performance of a 2 m LLA constructed in accordance to the CISPR 16-2-3 standard were made using

the numerical simulation in ref. [8]. The validation factor of the LLA was computed using a non-ideal current transformer model having $L_1 = 2.9 \ \mu H$, $L_2 = 2.8 \ mH$, $C_1 = 0$, $C_2 = 2.9$ fF, and $C_{IW} = 5$ pF. The validation factor is the response of the LLA to a folded dipole source which exhibits both a magnetic and an electric dipole moment. As can be seen from the data in Fig. 4, in positions 3 and 7 as described in Fig. C.7 of ref. [4] (electric dipole in plane of loop aligned for maximum excitation), the measured validation factor diverges near 30 MHz. This is due to the LLA responding to the electric dipole moment. It should be noted that what is plotted in Fig. 4 is the output voltage of the current transformer, which exhibits a nominal transimpedance of 1 Ω as specified in ref. [4] when connected to a 50 Ohm receiver. The current transformer employs a 25-turn secondary and an internal 50 Ω load such that the parallel combination of the internal load and the receiver gives a 1 Volt-per-Ampere response.

VI. CONCLUSIONS

The electric field response of the symmetric LLA is non-zero due to the finite common-mode rejection of the current transformer. The LLA necessarily generates a finite common-mode voltage at the secondary of the current transformer in response to an electric dipole; this behavior is fundamental and cannot be eliminated. A general model for a non-ideal LLA, including non-commensurate coaxial transmission lines, unequal terminating resistances, and a non-ideal current transformer, has been presented. Insertion of measured transformer 3-port scattering parameter data or an analytical model including inter-winding capacitance into the model used in ref. [8] predicts non-zero electric field response.

REFERENCES

[1] J. R. Bergervoet and H. V. Veen, "A large-loop antenna for magnetic field measurements," in *Proc. Zurich Int. Symp. EMC, 1989*, Zurich, Switzerland, Jan. 1989, pp. 29–34.

[2] M. Kanda, "A three-loop method for determining the radiation characteristics of an electrically small source," *IEEE Transactions On Electromagnetic Compatibility*, vol. EMC-26, no. 3, pp. 102–110, Aug. 1984.

[3] *CISPR 16-2-3 ed 2.0: Specification for radio disturbance and immunity measuring apparatus and methods Part 2-3: Methods of measurement of disturbances and immunity Radiated disturbance measurements*, IEC Std. 16-1-4, 2010.

[4] *CISPR 16-1-4 ed 3.0: Specification for radio disturbance and immunity measuring apparatus and methods - Part 1-4: Radio disturbance and immunity measuring apparatus - Antennas and test sites for radiated disturbance measurements*, IEC Std. 16-1-4, 2010.

[5] *EN 55015: Limits and Methods of Measurement of Radio Disturbance Characteristics of Electrical Lighting and Similar Equipment*, Austrian Electrotechnical Association Austrian Standards Institute Std., 2010.

[6] W. A. Pasmooij, "A Helmholtz large loop antenna system for improved magnetic field measurements," in *Proceedings of Eight International Conference on Electromagnetic Compatibility*, 1992, pp. 143–148.

[7] T. Shinozuka, A. Sugiura, and A. Nishikata, "Rigorous analysis of a loop antenna system for magnetic interference measurement," *IEICE Trans. Commun.*, vol. E76, no. 1, pp. 20–28, Jan. 1993.

[8] K. Takizawa, M. Midori, H. Kurihara, A. Nishikata, J. McLean, A. Medina, and R. Sutton, "A MoM analysis of validation factor for large loop antenna method," in *Proc. General Conference of IEICE*, Mar. 2014.

[9] J. S. McLean, "Balancing networks for symmetric antennas–I: Classification and fundamental operation," *IEEE Trans. Electromagnetic Compatibility*, pp. 503–514, Nov. 2002.